

STUDIES ON THE STRUCTURE OF FEATHER KERATIN

II. A β -HELIX MODEL FOR THE STRUCTURE OF FEATHER KERATIN

R. SCHOR *and* S. KRIMM

From the Harrison M. Randall Laboratory of Physics, University of Michigan, Ann Arbor. Dr. Schor's present address is Department of Physics, University of Connecticut, Storrs

ABSTRACT The assumption that the proline residues in feather keratin, which comprise 12 per cent of the total, are periodically located along the polypeptide chain is shown to lead to an essentially unique structure for this fibrous protein. The structure is based on a β -helix; *i.e.*, an extended chain which coils slowly to form a helix of relatively large pitch. Such helices tend to aggregate by hydrogen bonding to form cylindrical units, which in turn can aggregate further into cable-like structures. This model has been tested with respect to its predictions concerning the x-ray diffraction pattern, infrared spectrum, mechanical properties, and chemical behavior of feather keratin. Preliminary results indicate that it is better capable of accounting for the data than previously proposed structures.

INTRODUCTION

In a previous paper (1), we have considered the requirements which present experimental information imposes on a satisfactory model for the structure of feather keratin. Briefly, these are the following: (1) A 189 Å fiber axis identity period, with a pseudoidentity period half of this; (2) other characteristic fiber axis periodicities of 23.6₄ Å and 18.9 Å; (3) a meridian reflection at 2.96 Å, but none near 1.0 Å; (4) a characteristic 33 Å equatorial spacing; (5) perpendicular infrared dichroism for ν (NH); (6) the possibility of a small and limited extension on stretching; (7) the incorporation of about 12 per cent proline; (8) the breakdown of the structure into homogeneous units of molecular weight about 10,000. We wish to consider now in detail how a model previously proposed by us (2) satisfies these requirements.

β -HELIX HYPOTHESIS

As we have seen (1), x-ray diffraction and other data suggest that none of the presently known polypeptide chain conformations will satisfactorily account for the data on feather keratin. Although the structure is closely related to that of a β -protein, some deviation from the simple extended chain models is required, if only by the existence of long spacings. We wish to show that the introduction of essentially one assumption, *viz.*, a periodicity in the sequence of proline residues, suffices to generate a structure which is in reasonably good agreement with the data.

1. *Assumption of Periodic Proline Residues: β -helix Structure.* As we noted earlier, of the order of 12 per cent of the residues in feather are proline. Although the hypothesis of equivalence of residues (3) used in deriving other polypeptide chain conformations is a reasonable one for most amino acids, it does not seem likely that proline should be included among these. The presence of the ring structure associated with this imino acid would be expected to impose constraints on the conformation of the adjacent polypeptide chain which would not be true in the case of other amino acids. In fact, it has been estimated (4) that the presence of 8 per cent of proline randomly distributed in a polypeptide chain will prevent the chain from forming an α -helix. It is therefore not unreasonable to assume, which we will do, that the random distribution of about 12 per cent of proline in the polypeptide chain of feather keratin would not give rise to the highly ordered structure which is apparent from the x-ray diffraction pattern. If this is granted, then the simplest hypothesis is to assume that the proline residues are regularly spaced along the chain.

On this basis it now becomes possible to derive various characteristics of the polypeptide chain. Thus, if we take the projected amino acid repeat distance to be 2.96 Å, since this is the only appropriate meridian reflection in the proper region, then we conclude that there are 64 amino acid residues in the 189 Å identity period. According to the above hypothesis, the number of residues between successive prolines would therefore be restricted to 1, 3, 7, 15, 31, or 63. The corresponding percentages of proline are 50, 25, 12.5, 6.25, 3.13, and 1.56. The experimental data indicate about 11 per cent of proline in the whole calamus (1), and 13 per cent in the soluble unit (5). The hypothesis is therefore consistent with every eighth amino acid along the chain being proline. It is of interest to note that this result is consistent with preliminary amino acid sequence studies (6), in that no proline-proline sequences are found nor does proline occur more than once in the (admittedly few) tripeptides and tetrapeptides examined. Such a structural significance for proline is also supported by the observation (7) that the proline content is essentially constant between different parts of a feather and between feathers from different kinds of birds.

This periodicity in the proline residues accounts naturally for the very strong and persistent 8th order meridian reflection at 23.6₄ Å. The high intensity of this

reflection would result not only from the eightfold division of the identity period by the proline residues, but also as a consequence of three other factors: (1) The fixed spatial configuration of the ring carbon atoms should give rise to more coherent scattering than is true of the average side chain. (2) The free CO groups of the prolyl residues will probably each bind a water molecule, thus adding to the coherent scattering. (3) It is most likely that, in order to form the best hydrogen bonds and most regular structure, neighboring chains will align themselves with proline residues at the same level; this will further contribute to the strength of the 23.6₄ Å reflection. The persistence of this reflection follows from the fact that the periodicity is incorporated within the chain. Thus, disordering can begin in other parts of the chain without initial disruption of the proline to proline periodicity.

The local chain conformation between proline residues can be inferred from the following considerations. Taking the perpendicular dichroism of ν (NH) as 4.8:1 (8), and assuming a random orientation of the N–H dipoles about the fiber axis, each making an angle θ with this axis, then since this dichroic ratio is given by $\frac{1}{2}\tan^2\theta$, we find that the N–H dipoles must make an angle of at least 72.1° with this axis. If, as is likely, the true dichroic ratio is higher, then this angle would have to be larger. If we assume the polypeptide chain to be in one of the anti-polar conformations, then the most favorable possibility is the parallel-chain pleated sheet, which has an amino acid repeat that can be as low as 3.25 Å (9). Taking 72.1° as the minimum angle between the N–H dipoles and the axis, and assuming the chain direction to be perpendicular to the transition moment (which is closely enough true for this structure), we find the projected amino acid repeat to be 3.10 Å. This is higher than the values reported for the strong “meridional” reflection, *viz.*, 3.07 to 3.09 Å, and would be significantly more so for larger dichroic ratios. Of course, if we take the 2.96 Å meridional reflection to represent the projected amino acid repeat distance, then the parallel-chain pleated sheet is completely unacceptable. This is even more true of the anti-parallel-chain pleated sheet, which has an amino acid repeat of 3.50 Å (9). On the other hand, a polar chain conformation, such as the polar pleated sheet (10), is a possible basis for an acceptable structure since it has an amino acid repeat of 3.07 Å. A projected repeat of 2.96 Å can be achieved by tilting the chain axis about 15°, and the resulting dichroic ratio of over 6.7:1 is in quite satisfactory agreement with the experimental data. We will therefore assume that the chain conformation is that of a polar pleated sheet, or some small modification thereof.

We have to consider now the possibility of a longer range structure to the polypeptide chain. In view of the presence of a periodic sequence of proline residues, and since the proline introduces a small constraint even in an extended polypeptide chain, it is reasonable to expect that such a chain would take a helical form. This also provides the most natural way in which the residues acquire the tilt discussed in the previous paragraph. We designate such an extended chain which slowly coils

into a helical form as a β -helix. In the present case we will assume that the structure is basically a simple helix which makes one turn in 189 Å. It should be noted that this accounts in a natural way for the continuity between long and short spacings which is demonstrated by stretching experiments (1).

In the simple sheet structures composed of extended polypeptide chains, adjacent chains in the sheet are hydrogen-bonded to each other. If one chain is coiled slightly to form a helix, then there will be a tendency for a number of polypeptide chains to twist coaxially about the same axis in order to permit such characteristic hydrogen-bonding between chains to occur. It is as if a number of strands were twisted about each other to form a cable, with the bonding occurring in the cylindrical envelope of the structure. The result is that the polypeptide chains form a hollow cylinder, side chains projecting into and out of the cylinder, with the hydrogen bonds being roughly in the cylindrical surface. Possible parameters for such a structure in the case of feather keratin can be obtained as follows. If we consider an ideal β -helix structure, *i.e.*, neglect possible perturbations due to the proline residues, then the relationships between the pitch of the helix, P , the radius, r , the pitch angle, θ , the amino acid residue length along the chain, l , the number of chains m , the hydrogen-bonding distance between adjacent chains, d , and the number of residues per turn of the helix, n , are given essentially by:

$$P = 2\pi r \cot \theta \quad (1)$$

$$P/n = l \cos \theta \quad (2)$$

$$d = \frac{2\pi r \cos \theta}{m} \quad (3)$$

If we take $P = 189$ Å, $n = 64$, and $d = 4.75$ Å (9, 10) then we can compute θ , l , and r for a range of values of m . Results for several reasonable values of m are

TABLE I
POSSIBLE PARAMETERS OF A β -HELIX
MODEL FOR FEATHER KERATIN

m	θ°	l (Å)	r (Å)
8	11.6	3.02	6.19
9	13.1	3.04	7.00
10	14.5	3.06	7.83
11	16.1	3.08	8.67
12	17.6	3.10	9.34

shown in Table I. There is no unique way of determining at this stage the proper set of parameters for feather keratin, but several considerations indicate that $m = 10$ is a very compelling choice. First, it gives a value of l consonant with that obtained

from the best values of bond angles and distances in the polypeptide chain (11). Second, the presence of ten coaxial chains in the cylindrical unit would be expected to enhance the tenth, twentieth, *etc.* orders of the 189 Å repeat. As we have noted (1), the main fiber axis periodicity in addition to the 23.6₄ Å spacing is 18.9 Å (three orders of this spacing being quite intense), which is precisely that required by the $m = 10$ model. Third, the presence of ten chains and eight levels of proline residues in 189 Å leads to a pseudohalving of the structure; *i.e.*, there is essentially a repeat of the structure after five chains and four proline residues. This accounts nicely for the observation (1) that, whereas the identity period is 189 Å, most reflections fall on layer lines which are orders of 94.5 Å. Fourth, as we shall see later, a radial Fourier synthesis suggests that a structure of the above kind has a radius just under 8 Å. All these observations are most consistent with the ten-chain coaxial β -helical structure.

2. *Uniqueness of β -Helix Model.* It is of interest at this point to determine whether the assumptions which have been introduced lead to a unique model for the structure, or whether many different chain conformations are compatible with the proposed ten-chain coaxial helical structure. This problem has been studied with the aid of molecular models, both of the wire type (to a scale of 5 cm/Å) and the space-filling kind. The wire models consisted of planar peptide groups with the following dimensions: N-C' = 1.32 Å, C' -C _{α} = 1.53 Å, N-H = 1.01 Å, C _{α} -N = 1.47 Å, C' -O = 1.24 Å, N-H-C' = 123°, H-N-C _{α} = 114°, C _{α} -N-C' = 123°, N-C' -C _{α} = 114°, N-C' -O = 125°, and O-C' -C _{α} = 121°; tetrahedral carbon atoms with an angle of 109.5°, C _{α} -H = 1.09 Å, and C _{α} -C' = 1.54 Å; and planar trans proline residues which were regular pentagons of side 1.52 Å.

We consider first the case of a β -helical structure containing no proline, but in which corresponding amino acids on neighboring chains in the cylindrical complex are at the same z level. This permits the subsequent introduction of proline residues at the same level, which we are assuming will lead to optimum hydrogen-bonding and maximum regularity in the structure. For a given sequence of atoms along the polypeptide chain, *e.g.*, -CO-NH-CHR-, four helical structures are conceivable, based on whether the individual chains form right-handed or left-handed helices and on the orientation of, say, the CO groups on the polar chain. These four helical structures are: I. right-handed helix with CO groups pointed to the right, II. right-handed helix with CO groups pointed to the left, III. left-handed helix with CO groups pointed to the right, and IV. left-handed helix with CO groups pointed to the left. These four structures are not interconvertible by any translation and/or rotation. If we now require that optimum hydrogen bonding be associated with the most colinear $\begin{array}{c} \diagdown \\ \text{N-H} \cdots \text{O} = \text{C} \\ \diagup \end{array}$ configuration (12), then structures I and IV are immediately eliminated. This can be seen from Fig. 1, which shows the hydrogen bonding between corresponding amino acid residues on neighboring polar

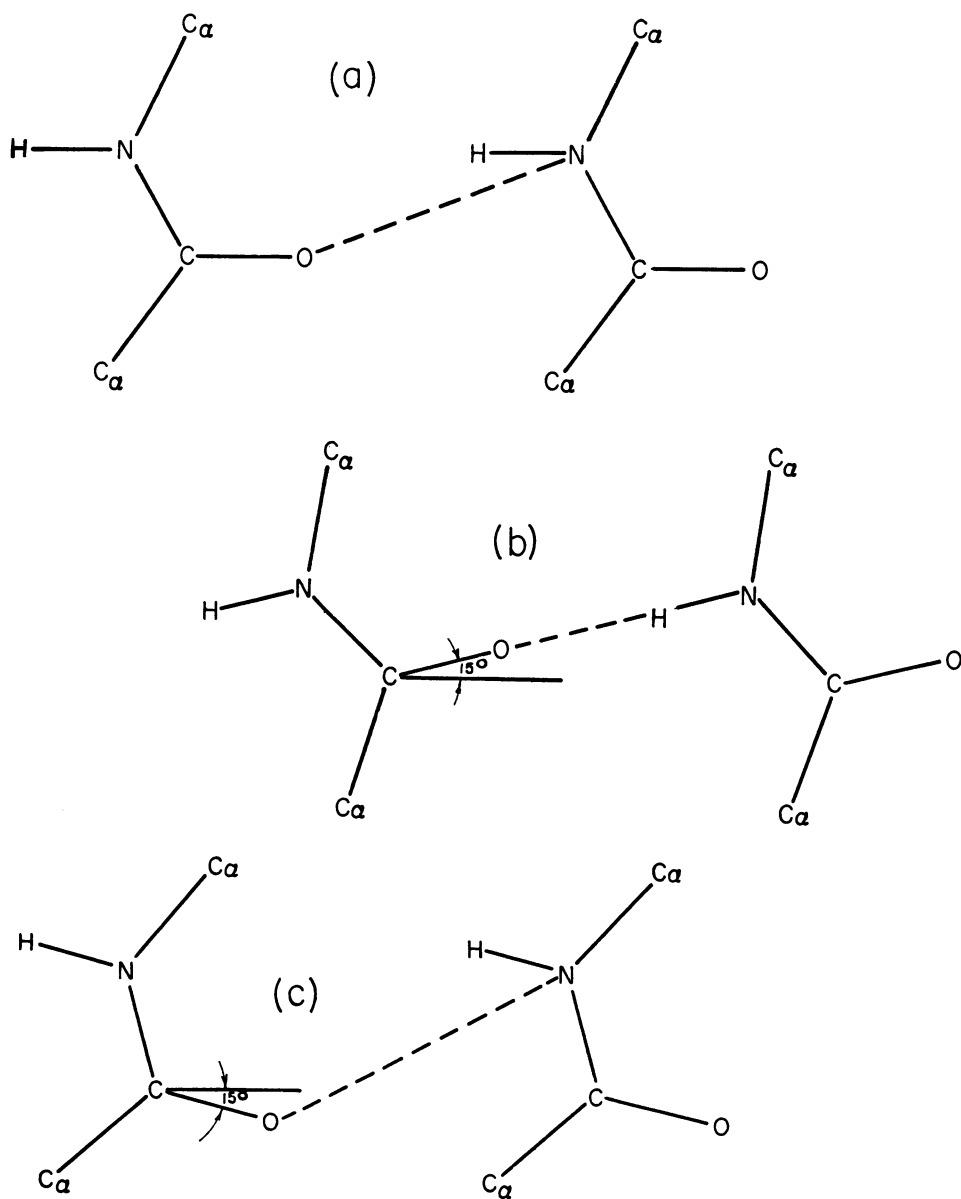


FIGURE 1 Hydrogen bonding between corresponding amino acids on neighboring polar chains. (a) Both amino acids oriented with chain axis vertical. (b) Both amino acids given a counterclockwise rotation of 15° . (c) Both amino acids given a clockwise rotation of 15° .

chains. Structures I and IV correspond to Fig. 1 *c*, which clearly gives unsatisfactory hydrogen bonds. On the other hand, structures II and III are compatible with the satisfactory hydrogen bond arrangement shown in Fig. 1 *b*. This bonding can be achieved with only a slight modification of the original form of the polar chain (10).

In Fig. 2 is shown a schematic diagram of the Pauling-Corey polar chain (10).

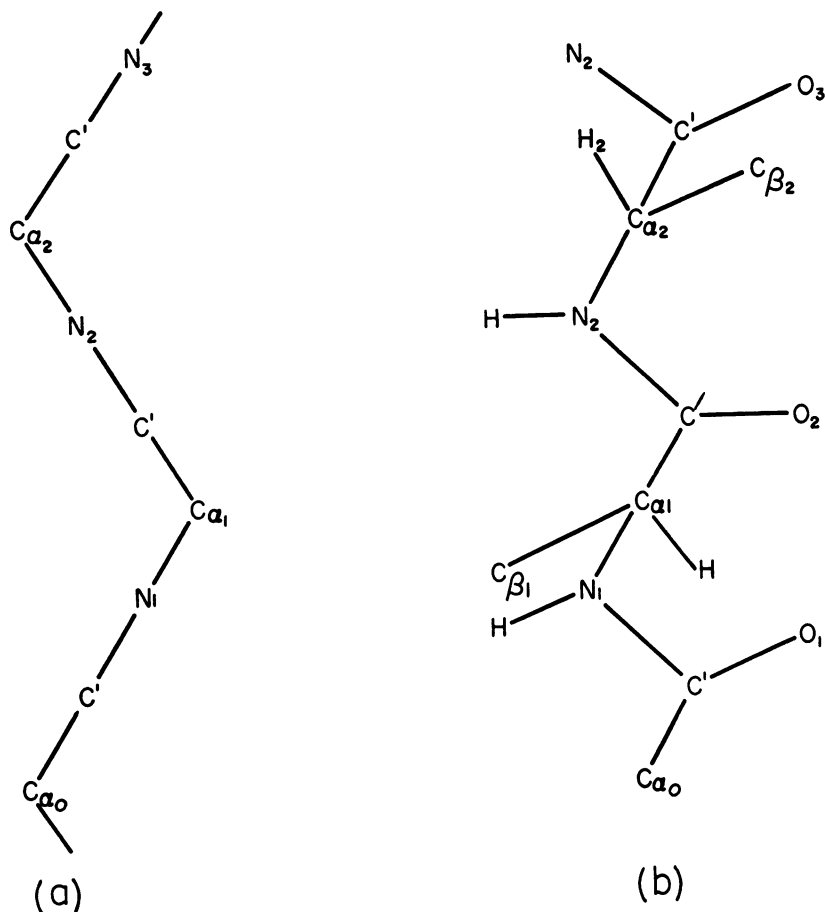


FIGURE 2 Schematic diagram of Pauling-Corey polar extended polypeptide chain. (a) Side view. (b) Front view.

In this structure the CO groups make an angle of about 8.5° with the perpendicular to the chain axis. It is possible to construct a closely related structure in which the CO groups are at right angles to the chain axis. Optimum hydrogen bonding is then achieved by tilting the chain axis by about 15° , as shown in Fig. 1*b*. (It is interesting to note that this tilt is of the order required by the ten-chain model; see

previous section and Table I.) This conformation differs from the original polar chain in the following manner: the $C_{\alpha_1}-C_{\beta_1}$ bond, which in the Pauling-Corey structure is coplanar with the preceding peptide group ($C'O_1N_1H$ in Fig. 2), is in the present structure about 10° below this plane (behind the plane of the figure) whereas the $C_{\alpha_2}-H_2$ bond is about 10° above the plane of the preceding peptide group. Such rotations are not expected to involve any significant increase in energy of the polypeptide chain (9, 12), so that the present conformation of the polar chain is an allowable one.

We now require that proline residues be introduced into this modified polar chain structure at every eighth amino acid site. It will be clear from Fig. 2 that there are two configurationally different amino acid residue sites. This results from the fact that one $C_\alpha-C_\beta$ bond, *viz.*, $C_{\alpha_1}-C_{\beta_1}$ is essentially *cis* to the preceding N-H bond, whereas the other corresponding bond, *viz.*, $C_{\alpha_2}-C_{\beta_2}$, is approximately *trans* to the preceding N-H bond. If we wish to insert a proline residue in a way that produces the least disruption in the chain conformation, it soon becomes clear that one of these sites is more favorable than the other. The molecular models show, and this can also be seen by reference to Fig. 2, that this is possible if the proline is inserted at C_{α_1} but not if it is inserted at C_{α_2} : the three-carbon ring of the proline residue fits easily between C_{α_1} , through C_{β_1} , to N_1 . No comparable ease of fit is possible at C_{α_2} ; in fact, the chain axis makes a bend of about 90° when the proline is inserted at C_{α_2} . The result of placing the proline residues in this more favorable position is that the proline rings (assumed to be at the same level on neighboring chains) are found, from molecular models, to be on the inside of the cylinder formed by structure II and on the outside of that formed by structure III.

The further evaluation of these structures now depends on the ability to construct satisfactory molecular models. When this is attempted, a preliminary investigation reveals that structure III has a serious defect which does not appear in structure II: some of the van der Waals contacts between neighboring peptide groups immediately following the proline residue in structure III are inadmissably short. In particular, if we consider the two such peptide groups on adjacent chains, it is found that the distance between a C_β on one chain and the H atom attached to C_α on the adjacent chain, H_α , is of the order of 1.5 Å. This distance is much too small (13), and can in no way be increased while retaining a polar chain conformation. These considerations thus eliminate structure III as a possibility.

The initial assumptions have therefore led to a unique β -helical ten-chain structure (assuming that it still can be built), other possibilities having been eliminated on the basis of either unsatisfactory hydrogen bonding or inadmissably poor van der Waals contacts.

3. Construction of a Molecular Model. It is now necessary to determine whether a satisfactory molecular model of structure II can be constructed. Aside from the usual requirements, such as planarity of the peptide group and satisfactory

bond angles and distances, an acceptable structure must satisfy conditions on hydrogen bond lengths and angles, and on van der Waals contacts.

With respect to the former, the requirements are reasonably clear. Most N-H...O hydrogen bond lengths, *i.e.*, the nitrogen to oxygen distance, fall in the range of 2.7 Å to 2.9 Å (14), and this requirement must be insisted upon in the structure. The conditions on the angle between the NH and NO vectors seem to be less certain. It was initially thought (3) that this angle should be no greater than 30°. Recent considerations (12) indicate that not only does greater stability result as the angle approaches 0°, but that the most stable configuration would be one in which the N, H, O, and C atoms are colinear. We have chosen the former condition as at least a minimal requirement while attempting to secure the latter.

The conditions defining the so called van der Waals contacts are not as clear cut. In the first place, quoted values for the van der Waals radii often differ significantly (13). Thus, the radius of hydrogen varies from 0.9 Å to 1.2 Å, that of oxygen from 1.2 Å to 1.4 Å. In the second place, the van der Waals radius is a function of the strength of the attractive and steric forces in the structure, and it is not always apparent that values obtained from the study of the structures of small molecules can be carried over directly to the case of large hydrogen-bonded molecules. Thus, although the sum of the usual van der Waals radii for carbon and oxygen is about 3.0 Å (15), the α -helix has carbon-oxygen contacts of 2.7 Å (16). Based on the α -helix (16), we have adopted as acceptable C...O contacts of 2.7 Å and C...C contacts of 2.9 Å. If the usual radius of oxygen, *viz.*, 1.4 Å (15), is used, it would be possible to accept a C...C contact of 2.6 Å (13). On the basis of a minimum value of the hydrogen radius of 0.9 Å (13), we can then accept C...H contacts of 2.2 Å and H...H contacts of 1.8 Å. These values are somewhat smaller than those derived from the usual van der Waals radii (15), but on the other hand energy requirements in other portions of a structure, involving for instance hydrogen bonds, may permit some close contacts without requiring the rejection of a structure.

The construction of a model of structure II was undertaken in two steps. In order to obtain a preliminary idea of the stereochemical feasibility of such a complex structure, the simpler problem of an ideal β -helix, *i.e.*, having no proline residues, was considered first. Then the introduction of proline residues was considered in terms of a "perturbation" of this simple model. In the case of the ideal β -helix, the asymmetric unit of structure consists of two amino acid residues, the remainder of the structure being derivable by symmetry considerations. It was possible to approach this problem by methods of analytical geometry, and in this way the coordinates of such a structure were obtained. They indicated that the structure could be built with essentially satisfactory hydrogen bonds and van der Waals contacts. Using initial coordinates from this structure, molecular models were then built which included proline residues. Insertion of these required some variations to be made in

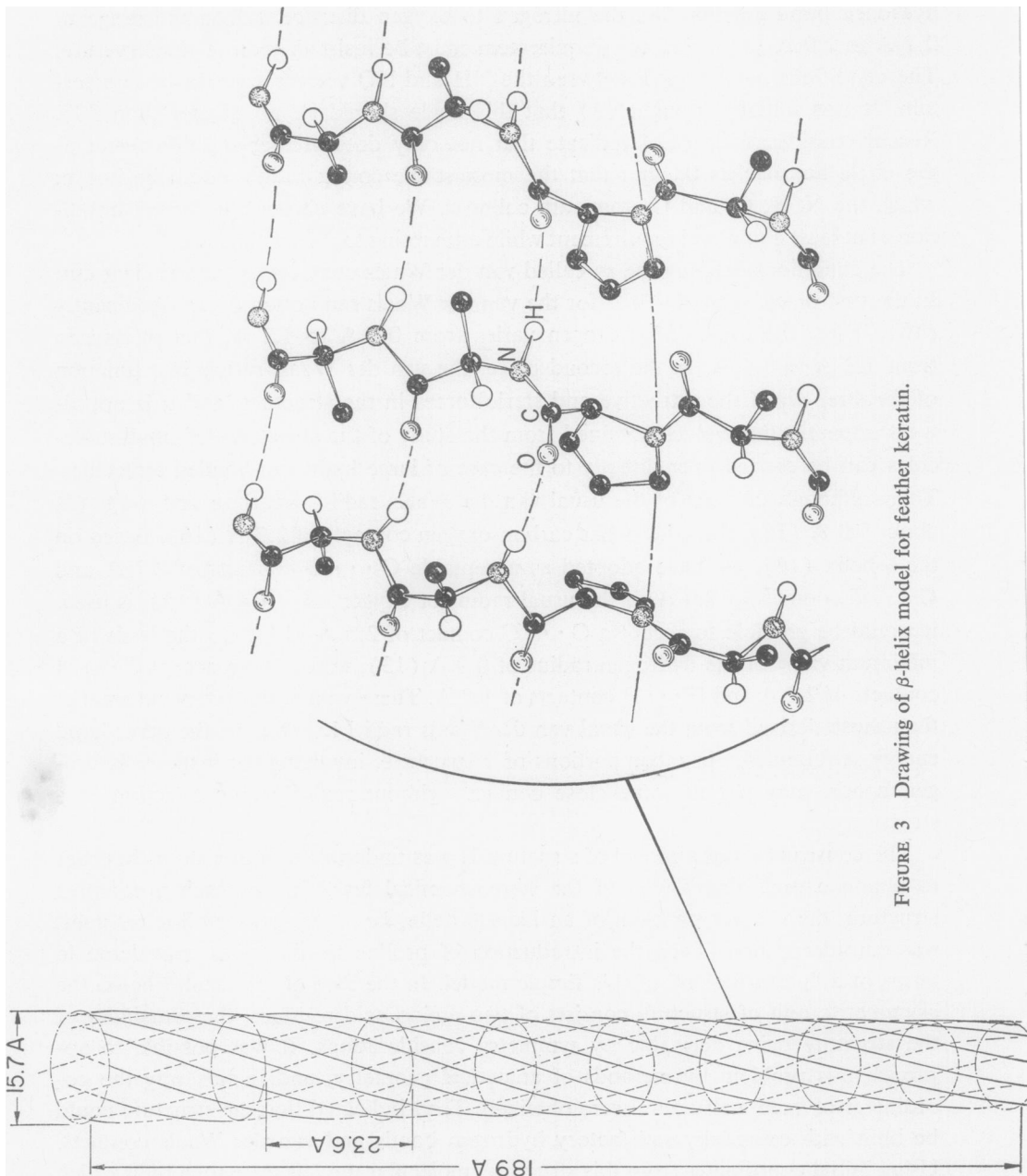


FIGURE 3 Drawing of β -helix model for feather keratin.

the parameters of the ideal model, but none of these was serious. A sketch of this model is shown in Fig. 3, and rough coordinates (accurate to about ± 0.1 Å) are given in Table II.

The model satisfies hydrogen-bonding criteria in that all bond lengths are in the range of 2.7 Å to 2.9 Å and the angle between NH and NO vectors is always less

TABLE II
ROUGH COORDINATES FOR ATOMS IN β -HELIX
MODEL OF FEATHER KERATIN

Atom	x (Å)	y (Å)	z (Å)	r (Å)	φ°
$C_{\alpha 1}$	3.9	5.3	0.0	6.6	8.0
C_1'	4.6	6.1	1.1	7.7	7.5
O_1	5.7	5.8	1.5	8.2	0.0
N_1	3.9	7.1	1.5	8.1	16.0
H_1	3.0	7.3	1.2	7.9	22.5
$C_{\alpha 2}$	4.4	8.1	2.6	9.2	16.0
C_2'	3.7	7.8	3.9	8.7	19.5
O_2	3.5	8.8	4.7	9.4	22.5
N_2^*	3.3	6.6	4.1	7.4	18.5
$C_{\alpha 3}^*$	2.6	6.1	5.3	6.7	22.0
C_3'	3.1	7.0	6.5	7.7	20.5
O_3	4.3	6.9	6.8	8.2	12.5
N_3	2.3	7.8	7.0	8.1	28.5
H_3	1.3	7.9	6.7	8.0	35.5
$C_{\alpha 4}$	2.6	8.7	8.1	9.1	28.0
C_4'	2.9	7.8	9.3	8.3	24.5
O_4	4.0	7.5	9.5	8.5	16.0
N_4	1.8	7.4	9.9	7.6	31.0
H_4	0.9	7.7	9.7	7.8	38.0
$C_{\alpha 5}$	1.9	6.5	11.1	6.8	28.5
C_5'	2.2	7.4	12.3	7.7	28.0
O_5	3.4	7.7	12.7	8.4	21.0
N_5	1.1	7.9	13.0	7.9	36.5
H_5	0.2	7.6	12.7	7.6	43.5
$C_{\alpha 6}$	1.2	8.7	14.2	8.8	37.0
C_6'	1.6	7.9	15.4	8.1	33.5
O_6	2.7	7.8	15.8	8.2	25.0
N_6	0.5	7.4	16.1	7.5	40.5
H_6	-0.5	7.6	15.8	7.6	48.0
$C_{\alpha 7}$	0.6	6.7	17.3	6.7	39.0
C_7'	0.7	7.6	18.6	7.6	39.0
O_7	1.8	8.0	19.0	8.2	32.0
N_7	-0.5	7.8	19.1	7.8	48.0
H_7	-1.3	7.5	18.8	7.6	54.5
$C_{\alpha 8}$	-0.6	8.7	20.4	8.7	47.5
C_8'	-0.2	8.0	21.7	8.0	46.0
O_8	0.9	8.1	22.1	8.2	38.0
N_8	-1.2	7.2	22.2	7.3	53.5
H_8	-2.1	7.1	21.8	7.4	61.0

* Proline ring.

than 30° . As for van der Waals contacts, most are satisfactory although some are a bit short. All $C \cdots O$ contacts are 2.7 Å or greater, as required. For the three interior amino acids other than proline in the eight amino acid asymmetric unit the $C_\beta \cdots H_\alpha$ contacts between neighboring chains are about 2.0 Å, some 0.2 Å smaller than would be desirable. If the γ carbon atom of the proline ring is allowed to be 0.4 Å below the plane of the ring, as in L-leucyl-L-prolyl-glycine (17), then $C \cdots C$ contacts of at least 2.6 Å can be achieved. There are some short contacts between hydrogen atoms on adjacent proline rings: $H_\alpha \cdots H_\gamma = 1.4$ Å and $H_\beta \cdots H_\gamma = 1.4$ Å. These results are based on a symmetric proline ring with sides of 1.52 Å. It might be noted that in the above tripeptide (17) the proline ring is not symmetrical and the ring bond lengths are less than 1.52 Å: 1.45 Å, 1.46 Å, 1.50 Å, 1.51 Å, and 1.50 Å. These modifications would somewhat improve the above short contacts.

One general feature of the proposed model is that the axial projections of all amino acid residues are not the same. The projections of the proline residues and the residues near the proline groups are somewhat smaller than those of the remaining amino acid residues. Thus the proposed structure deviates from an ideal β -helix. The general consequences of this will be considered later.

It is difficult to assess the significance of the short contacts in determining the acceptability of the proposed molecular model. In the first place, a more detailed investigation of the model was deferred until it could be ascertained that the general features of the structure were in accord with experimental data. Secondly, the dimensions assumed for the wire models may not have allowed a reasonable flexibility in the construction of the molecule. Thus, for example, the tetrahedral angle was taken as 109.5° , although this angle is known to range up to 118° (17). It is entirely possible that, with the allowance of such small distortions in and between the polypeptide chains, a satisfactory compromise between strong hydrogen bonds, minimal bond angle distortions, and slight overlap of atomic radii would still result in a stable structure.

We will tentatively assume that a satisfactory molecular model of structure II can be built, and will now examine the extent of agreement between this model and the experimental data.

EVALUATION OF THE β -HELIX HYPOTHESIS

The assumption of a regular sequence of proline residues along the polypeptide chain of feather keratin has led, as we have seen, to a unique structure of which it is possible to construct an initially satisfactory model. It is desirable at this point to evaluate the ability of this model to account for the experimental data. In particular, we are interested in explaining at least the main features of the x-ray diffraction pattern as well as the other physical and chemical characteristics manifested by feather keratin (1).

1. *Equatorial Diffraction Pattern.* The equatorial diffraction pattern is determined by the projected electron density distribution on a plane perpendicular to the fiber axis. Since reasonable approximations to the projected density could be obtained even in the absence of a refined model, an attempt was first made to investigate the ability of the model to account for the equatorial pattern.

As we have seen, the proposed model approximates a cylinder of radius about 8 Å. If we assume that the side chain residues extend approximately 3 Å beyond the main chain, then the diameter of the proposed cylindrical unit is about 22 Å. If such units are to account for the prominent 33 Å and 50 to 55 Å equatorial reflections, then it is clear that they cannot be acting singly, *e.g.*, in hexagonal close-packing, but must be aggregated into larger units. This is not unreasonable in view of the known -S-S- and salt linkages between polypeptide chains which determine the secondary and tertiary structure of proteins. We have examined aggregates of three cylinders, but find that no packing arrangement of them gives a reasonable accounting of the equatorial diffraction pattern. On the other hand, aggregates of seven cylindrical units do have many diffraction features in common with the observed results. (We have also tried various forms of a proposed cylindrical lattice (18), but without any success.)

We assume that seven cylindrical units, a "cable," aggregate with their axes parallel to one another. These are shown in Fig. 4 in one possible packing arrangement. The diameter of one of these cables is taken to be 67.2 Å, which is consistent with the dimensions discussed in the previous paragraph. We have computed the intensity transform of the isolated cables on the assumption that the cylindrical

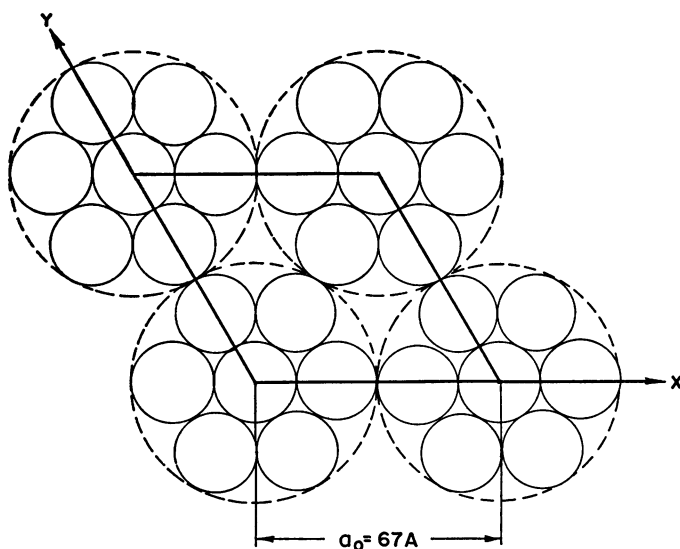


FIGURE 4 Packing arrangement of seven-cylinder aggregates.

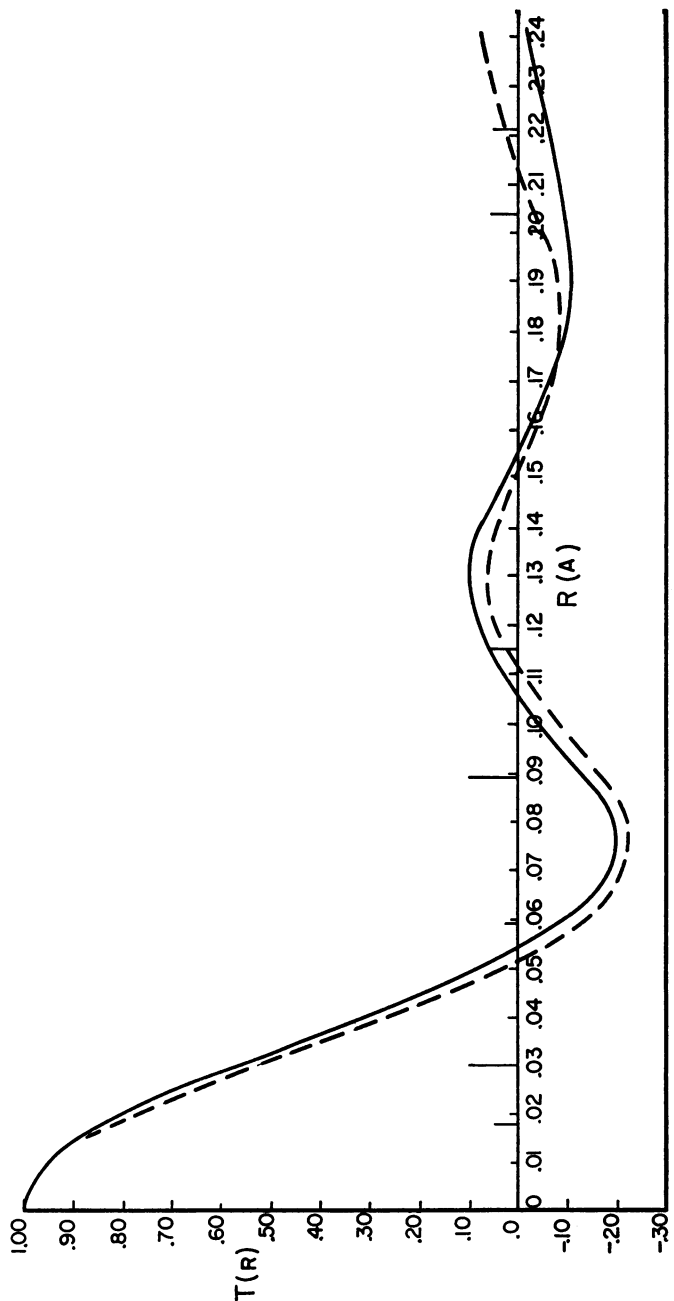


FIGURE 5 Equatorial transforms of approximations to the cylindrical unit of structure. —, structure A; ---, structure B (see text for details on these structures).

unit could be approximated by a hollow cylinder of $r = 8$ Å, weighted one-half (representing the main chains), and a uniform shell from $r = 3$ Å to $r = 11.2$ Å, weighted one-half (representing the side chains). This is certainly a zeroth approximation to the projected structure, but several of the main features of the equatorial pattern are seen to emerge, *viz.*, strong reflections near 35 Å and 11 Å and a weaker reflection near 17 Å. The intensity transform of the isolated cable is not strong in the 50 Å region nor near 8.8 Å, but does show a moderate peak near 7.3 Å and a weaker peak near 5.6 Å.

The equatorial diffraction pattern of the hexagonal lattice shown in Fig. 4 was computed for two different approximations of the projected electron density of the cylindrical unit. Structure A approximates the projected electron density by a hollow cylinder of $r = 7.83$ Å weighted one-half to represent the main chains, and three hollow cylinders of $r = 3$ Å, $r = 5$ Å, and $r = 10$ Å weighted one-eighth, one-eighth, and one-quarter, respectively, to represent the side chains. Structure B approximates the projected electron density by a hollow cylinder of $r = 8$ Å weighted one-half, and two hollow cylinders of $r = 5$ Å and $r = 10$ Å weighted one-quarter each. In addition, 5 per cent of the scattering power for structure B was assumed to be water located uniformly at $r = 3$ Å. (Infrared spectra indicate the presence of about this much bound water in feather keratin.) The transform of a cylindrical unit, F_c , was then evaluated as the sum of the transforms of the above cylinders, each given by $J_0(2\pi rR)$, J_0 being the zero order Bessel function, r the radius of the cylinder, and R the radial coordinate in reciprocal space. The resulting transforms of the two structures are shown in Fig. 5. The transform of the lattice shown in Fig. 4 is then given by

$$F_T(hk0) = F_c(R_{hko})G_{hko} \quad (4)$$

where G_{hko} is the structure factor for a set of points located at the unit cell coordinates (0,0), (1/3,0), (2/3,0), (1/3,1/3), (2/3,2/3), (0,1/3), and (0,2/3), and

$$R_{hko} = \frac{1}{d_{hko}} = \frac{1}{67.2} \sqrt{\frac{4}{3} (h^2 + hk + k^2)}.$$

The intensities were taken as proportional to F_T^2 multiplied by the multiplicity factor for the planes involved; Lorentz and polarization corrections were computed to be small and were therefore omitted. The results of the calculation for the stronger reflections are shown in Table III.

The agreement between calculated and observed reflections, while not perfect, is not grossly out of line, and in fact is comparable with that obtained with other fibrous protein structures. The strong reflections at ~ 55 Å, 33 Å, and 11 Å are accounted for, as well as some of the weaker reflections. The observed intensity at about 4.6 Å is difficult to determine because of the overlap of scattering from the non-crystalline component. The major difficulties are the absence of an observed

TABLE III
EQUATORIAL REFLECTIONS OF PROPOSED FEATHER STRUCTURE

Reflection	Spacing (A)	Intensity		Observed		
		Structure A	Structure B	Spacing	Intensity	
100	58.0	4152	4020	~55	s	
110	33.5	7380	6840	33.5	vs	
200	29.0	1134	1056			
300	19.4	264	264			
220	16.8	216	288	17.1	mw	
410	12.7	1740	2328			
330	11.2	5370	8520	11.2	s	
600	9.65	66	594			
610	8.85	—	—	8.84	w-m	
630	7.30	4764	1776			
900	6.43	—	120			
660	5.58	2640	1980	5.8	w	
930	5.36	6240	3300			
12,00	11,20 } 770 860 }	~4.82	910	494	4.9	m
770						
10,40		4.67	284	—	4.66	m (?)
11,30	13,00 } 870 960 }	~4.50	204	145	4.50	w
870						

vs = very strong, s = strong, m = medium, w = weak.

reflection at 8.8 A and the prediction of an unobserved reflection at about 7.3 A. When we recall the crudeness of the approximation to the projected electron density which was used, it is not surprising that the agreement is not better than it is. As seen from Table III, the predicted intensities of some of the reflections are sensitive to the approximation used, so that it may be surmised that the discrepancies could be reduced in a more accurate approximation to the model. This is also true of the spacings, which are based on a simple hexagonal cell. Finally, our present computations were based on a particular packing arrangement of the cables. Deviations from this arrangement would undoubtedly affect the predicted intensities. We feel that at the present stage of the analysis it can be said that the proposed model is basically capable of explaining the equatorial diffraction pattern of feather keratin, although not all the details have been resolved.

2. *Radial Fourier Synthesis.* In the above we have been concerned with calculating the diffraction pattern to be expected from the proposed structure and comparing it with the observed pattern. We may also inquire about the inverse procedure, *viz.*, obtaining the electron density distribution directly from the observed pattern. In this case we are frustrated not only by the usual lack of knowledge of the phases of the reflections, but also by the fact that a fiber diagram provides the

cylindrically averaged intensity transform. It may, however, be possible to obtain information on the cylindrically averaged radial electron density distribution, which can be of help in evaluating a structure.

We consider first the case of a cylindrically symmetric structure. The projected electron density is given by

$$\rho(r) = \int_{-\infty}^{+\infty} \rho(r, z) dz = \int_{-\infty}^{+\infty} \left[\int_{-\infty}^{+\infty} \int_0^{2\pi} \int_0^{\infty} F(R, \zeta) e^{2\pi i (R \cdot r + z\zeta)} R dR d\psi d\zeta \right] dz \quad (5)$$

In this equation $\rho(r, z)$ is the electron density at the point specified by the cylindrical polar coordinates (r, z) , $F(R, \zeta)$ is the transform at a point in reciprocal space specified by a radial coordinate, R , and an axial coordinate, ζ , and ψ is the angular coordinate in reciprocal space. The integral over z is a delta function, $\delta(\zeta)$. Performing the integral over the angular coordinate, we then obtain:

$$\rho(r) = 2\pi \int_0^{\infty} F(R, 0) J_0(2\pi r R) R dR \quad (6)$$

In the usual case of discrete reflections the integration may be replaced by a summation, so that, apart from a factor of 2π , we have:

$$\rho(r) = \sum_R R F(R, 0) J_0(2\pi r R) \quad (7)$$

The usual difficulty in solving equation (7) for $\rho(r)$ is the lack of knowledge of the phases (in this case the signs) of F .

Consider next the case of a structure which is not cylindrically symmetric. The projected electron density is

$$\rho(r, \alpha) = \int_{-\infty}^{+\infty} \rho(r, \alpha, z) dz = \int_0^{2\pi} \int_0^{\infty} F(R, \psi, 0) e^{2\pi i r R \cos(\alpha - \psi)} R dR d\psi \quad (8)$$

where the integration over z has already been done. If this structure occurs in the specimen with random orientation about its axial direction, then we can obtain an average radial electron density distribution:

$$\overline{\rho(r)} \equiv \frac{1}{2\pi} \int_0^{2\pi} \rho(r, \alpha) d\alpha = \int_0^{\infty} R \overline{F(R, 0)} J_0(2\pi r R) dR \quad (9)$$

where

$$\overline{F(R, 0)} \equiv \frac{1}{2\pi} \int_0^{2\pi} F(R, \psi, 0) d\psi \quad (10)$$

Again, when the reflections are discrete:

$$\overline{\rho(r)} = \sum_R R \overline{F(R, 0)} J_0(2\pi r R) \quad (11)$$

Equation (11) is similar to equation (7) except for the replacement of $F(R, 0)$ by $\overline{F(R, 0)}$.

In order to use equation (11) we must not only know the phases of the $\overline{F(R, 0)}$,

but we must know how to obtain $\overline{F(R, 0)}$ from the observed intensities, $I(R, 0)$. Let us assume that the structure is centrosymmetric, so that $F(R, \psi, 0) = F^*(R, \psi, 0)$. Then:

$$I(R, 0) = \frac{1}{2\pi} \int_0^{2\pi} F^2(R, \psi, 0) d\psi \quad (12)$$

If we use Schwartz's inequality:

$$\left| \int fg d\tau \right|^2 \leq \int |f|^2 d\tau \cdot \int |g|^2 d\tau \quad (13)$$

and let $f = F(R, \psi, 0)$ and $g = 1$, then:

$$\left| \int F(R, \psi, 0) d\psi \right|^2 \leq 2\pi \int_0^{2\pi} F^2(R, \psi, 0) d\psi \quad (14)$$

From equation (12) it then follows that:

$$|\overline{F(R, 0)}|^2 \leq I(R, 0) \quad (15)$$

The equality sign in Schwartz's inequality holds only if f and g are directly proportional, which would be true only if $F(R, \psi, 0)$ were independent of ψ . Since this is not the case in the present instance, the magnitude of $\overline{F(R, 0)}$ is determinable from the observed intensities only to within the limits established by equation (15), *viz.*, $|\overline{F}|$ is never greater than \sqrt{I} . This would seem to limit the applicability of equation (11). However, $\overline{\rho(r)}$ is much more sensitive to the choice of signs than to the magnitudes of $\overline{F(R, 0)}$, so it may reasonably be expected that the main features of $\overline{\rho(r)}$ will emerge even if the magnitudes are equated to \sqrt{I} . This would be especially true of structures approximating cylindrical symmetry.

In order to determine $\overline{\rho(r)}$ from equation (11) it is necessary to know the signs of $\overline{F(R, 0)}$. It has not been possible to determine these experimentally because of the inability to achieve an isomorphous replacement with feather. Similarly, without prior knowledge of the size and shape of the fundamental scattering unit, it is not possible to utilize the minimum wavelength method (19) unambiguously. However, an analogy to the latter method may provide a possibility for a sign determination. We are interested in determining the continuous transform of the fundamental unit of structure. For this purpose it is necessary to know the regions of maximum scattering and the nodal regions in the equatorial transform. The first node in the transform undoubtedly occurs near $R = 0.06 \text{ \AA}^{-1}$, which is consistently weak in the x-ray diffraction pattern (1). This is supported by the evidence (20) that the $R = 0.03 \text{ \AA}^{-1}$ equatorial reflection can be moved to $R = 0.024 \text{ \AA}^{-1}$ without significant intensity changes, thus indicating that it probably lies within the first maximum of the transform. On this basis, the reflection at $R = 0.089 \text{ \AA}^{-1}$, and possibly that at $R = 0.115 \text{ \AA}^{-1}$, are to be given a negative sign. The next node is most likely near $R = 0.12 \text{ \AA}^{-1}$. This follows not only from the absence of reflections

immediately beyond, but from the observation (1, 21) that when, upon treatment with water, the $R = 0.115 \text{ \AA}^{-1}$ spot moves to slightly lower R values, its intensity increases. We now find an extended region, roughly from $R = 0.12 \text{ \AA}^{-1}$ to $R = 0.20 \text{ \AA}^{-1}$, in which only one very weak reflection, at about $R = 0.17 \text{ \AA}^{-1}$, is observed. If the transform follows the general form that it has thus far exhibited, with essentially the same wavelength, then we expect it to become less negative in the region of $R = 0.12 - 0.20 \text{ \AA}^{-1}$ (perhaps not actually crossing the axis to become positive) and then more negative beyond. This would suggest assigning a negative sign to the $R = 0.215 \text{ \AA}^{-1}$ reflection. Using the above sign combination, with the $R = 0.059 \text{ \AA}^{-1}$ reflection being negative, we have computed $\overline{\rho(r)}$ from equation (11), taking $|\overline{F(R, 0)}| = \sqrt{I}$. The result is shown in Fig. 6, where curves are shown in

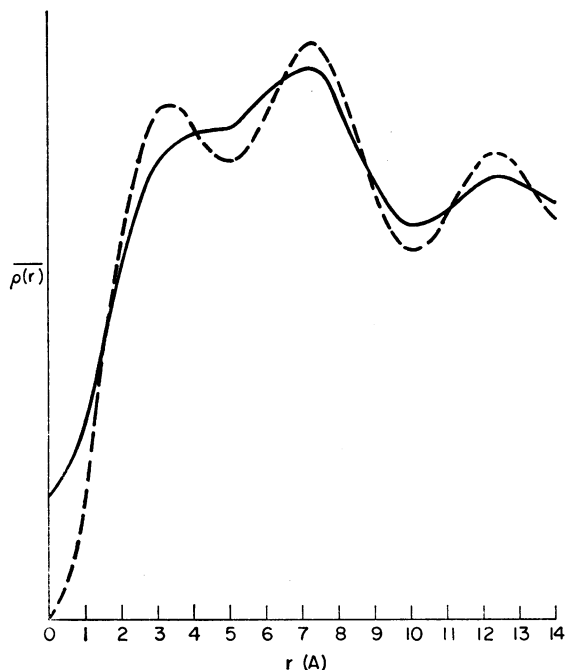


FIGURE 6 Radial Fourier of feather keratin. —, non-crystalline contribution to 4.66 \AA reflection taken as 0.5; ---, non-crystalline contribution to 4.66 \AA reflection taken as 0.0.

which the measured intensity of the 4.66 \AA reflection was used, and in which this reflection was diminished by a factor of two to allow for the contribution of the non-crystalline component in this region.

The average radial electron density distribution shown in Fig. 6 is in good agreement with that predicted by the proposed model. The density is low at $r = 0$, the axis of the cylindrical unit. It builds up to a small maximum at $r = 3 \text{ \AA}$ to 4 \AA ,

where we would expect the side chains to begin to contribute. The main maximum is near $r = 7.5 \text{ \AA}$, corresponding to the radius at which the main chain atoms are located. The density then falls off and subsequently rises to a small peak at about $r = 12.5 \text{ \AA}$, where we expect the contributions of neighboring cylindrical units to become evident. The radial Fourier synthesis, although it still involves some ambiguity about the signs of the reflections, is consistent with a general model of the type proposed.

3. *Meridional Diffraction Pattern and Cylindrical Patterson Function.* The complete analysis of the meridional diffraction pattern of the proposed model is difficult at this stage because of (a) the relatively approximate coordinates of the main chain atoms, (b) the uncertainties in the positions of atoms in the side chains, and (c) the necessity of including the scattering contribution of neighboring units. Nevertheless, a preliminary evaluation can be made in order to see whether some of the main features in the diffraction pattern can be accounted for.

As we noted earlier, the periodicity in the proline residues along the chain can account for the very strong 8th order meridian reflection, at 23.6 \AA , and the weak 16th order reflection which is observed. This follows from the presence of eight asymmetric units in the helical repeat, which, according to helix transform theory (22), imposes the following selection rule on the orders, n , of the Bessel functions which can occur on any layer line of index l :

$$n + 8m = l \quad m = 0, \pm 1, \pm 2, \dots \quad (16)$$

Thus, meridian reflections, which correspond to $n = 0$, can occur only on layer lines whose index is a multiple of eight. The rapid decrease in intensity of this sequence, only $l = 8$ and $l = 16$ being observed, can be understood in terms of the extended region (comprising several angstroms in z) responsible for this scattering. This results in a more rapid fall-off of scattering factor with increasing scattering angle than is true for individual atoms.

The proposed model has sixty-four amino acid residues in the 189 \AA repeat of the helix, and we therefore expect to find a meridional reflection at 2.96 \AA . That this reflection is weaker than might be anticipated could be due to the fact that in the structure 2.96 \AA represents only the average axial projection of an amino acid. As we noted in discussing the model, the proline residues introduce discontinuities in the chain such that the axial projection of some amino acid residues is larger than 2.96 \AA and that of others smaller. This would be expected to result in a relative weakening of the 2.96 \AA reflection. The model can also account for the absence of the meridional reflection near 1.0 \AA which is usually found in the β -proteins. In the latter this reflection arises from the approximately equal axial projection of the successive atoms in the peptide group of the extended polypeptide chain. In the present model the residues are tilted with respect to the fiber axis so that the C', O, and N atoms in a peptide group are essentially in one horizontal plane; nor do the

atoms in the peptide group and the C_α atom form the regular sequence along the chain which is true of the β -sheet structures. It is therefore to be expected that this reflection will be significantly weaker in the proposed model. As was observed earlier, the presence of ten polypeptide chains in the cylindrical unit of structure, resulting in a pseudotranslation of one-tenth the identity period, can account for the enhancement in the 10th, 20th, and 30th orders of the 189 Å identity period. Also, the model repeats after a fiber axis translation of 94.5 Å as a result of the ten-chain eight-proline structure. This explains quite nicely why most reflections are orders of 94.5 Å. The fact that several odd orders of 189 Å are observed indicates that there is a departure from perfect translational symmetry.

The agreement for other aspects of the meridional diffraction pattern is not so favorable. Thus, if there were strict tenfold rotational symmetry then there would be an additional selection rule on n (22), *viz.*,

$$n = 10k \quad k = 0, \pm 1, \pm 2, \dots \quad (17)$$

This would impose a restriction on the Bessel functions that could occur on a given layer line which is not evident in the observed pattern. There are various factors, however, which probably interfere with the presence of a strict rotational symmetry: the side chains of neighboring polypeptide chains need not correspond, and packing of the cylindrical units most likely gives rise to small distortions from the ideal symmetry (23). The selection rule indicated by equation (17) therefore is probably relaxed. The strong reflections corresponding to fiber axis spacings of 6.30 Å and 3.15 Å are not accounted for by the backbone of the structure. They do, however, correspond to periodicities associated with the side chains, although the fine structure of these reflections remains to be explained in greater detail. In particular, since the side chains are less strongly related to each other by symmetry (because of the possibility of free rotation, and therefore the existence of many conformations), there will in general be a relaxation in the restrictions on the orders of the Bessel functions which they contribute on any given layer line, so that meridional and near-meridional reflections will be permitted. The other strong reflection, at 4.97 Å on the meridian, does not appear to be related to any obvious periodicity in the proposed structure. It may arise as a result of distortions from the ideal structure, similar to the situation found in some synthetic polypeptides (23).

The cylindrical Patterson function of the proposed structure has been computed, and is shown in Fig. 7. The effect of side chains has been neglected, and each amino acid residue has been approximated by a point and given an equal axial projection. Intrachain vectors, indicated by crosses, occur along line A; interchain vectors are found along lines B₊ and B₋, C₊ and C₋, etc. Proline residues are indicated by a P. Comparison with cylindrical Patterson functions obtained from the experimental data (1) indicates several areas of agreement. Thus, strong peaks are found near the $(r, 0)$ regions marked I and II in Fig. 7, and near $(0, 19)$ and

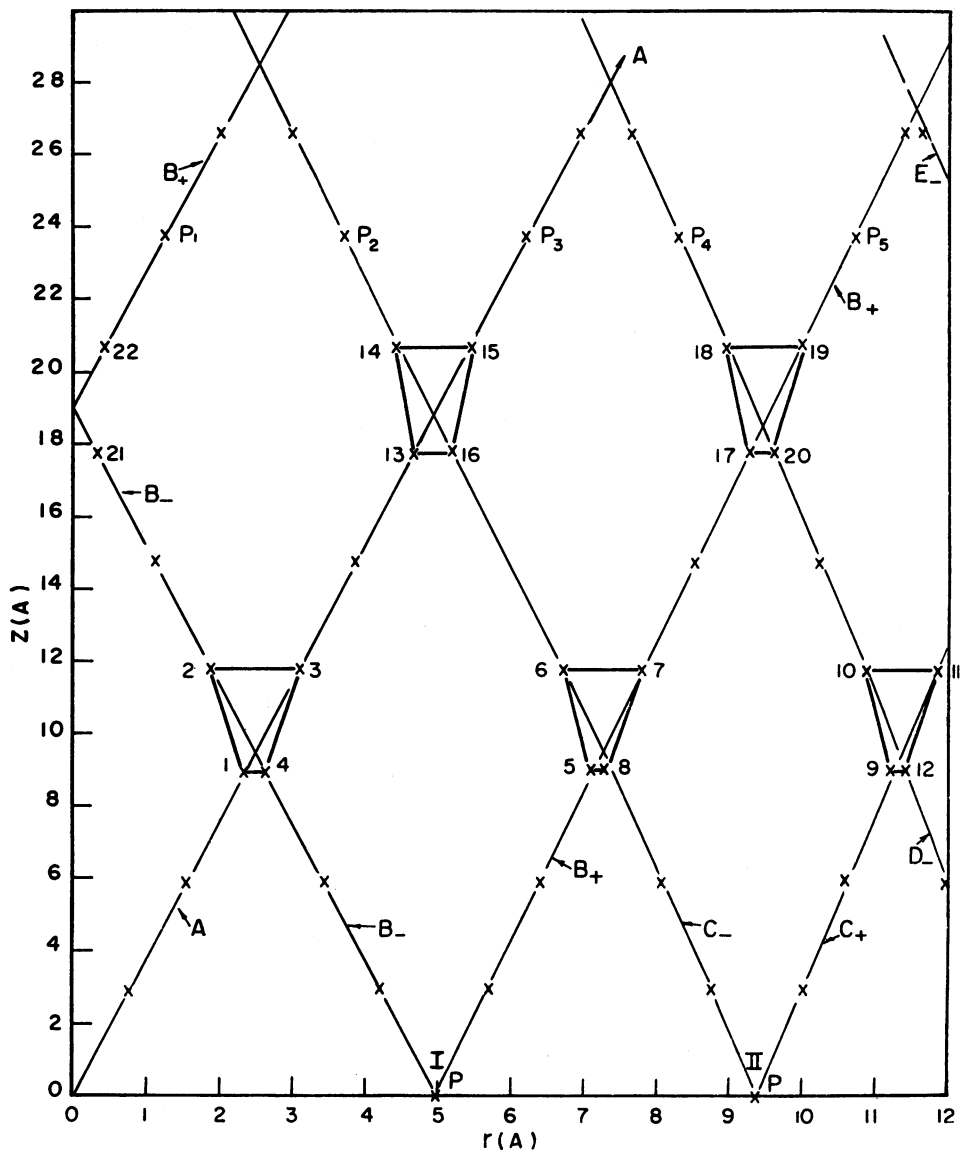


FIGURE 7 Cylindrical Patterson function for idealized unit of proposed feather keratin structure.

(0, 24). Although the latter peak is predicted nearer (1.2, 24), it is probable that the resolution in the experimental Patterson is not good enough to verify this. Peaks are also found in the experimental Patterson near the quadrilaterals (1, 2, 3, 4), (13, 14, 15, 16), and (17, 18, 19, 20), although none is found to correspond to the other comparable regions in Fig. 7 where an overlap of several vector peaks

might be expected to stand out. Nor does the calculated Patterson predict the peak near (0, 14) which is found. The agreement between predicted and observed Pattersons, while comparable to or better than that obtained for other fibrous structures (24), is still not complete. A more detailed model will probably have to be used in obtaining the calculated Patterson before the extent of agreement can be tested in greater detail.

In sum, the model predicts several of the main features of the meridional diffraction pattern and the cylindrical Patterson of feather keratin, but does not as yet account for others. In part this may be due to the uncertainties and approximations which were introduced into the calculations. It may also arise from factors which have not been taken into account, such as the presence of distortions from helical symmetry which exist in the structure. It is felt, however, that the extent of agreement which is achieved warrants the retention of the proposed model as a satisfactory preliminary approach to the structure of feather keratin.

4. *Chemical and Other Properties.* We will consider now the ability of the proposed model to account for various other properties exhibited by feather keratin.

(a) *Effect of Stretching.* Feather can be stretched about 6 per cent, accompanied by a general increase in all its meridional spacings of about the same amount with no corresponding change in the equatorial spacings (1). Beyond this point the specimen breaks. Although various treatments lead to a contraction of the feather (20), none has been found to allow an extension much beyond that indicated above. We have found this to be true even after disruption of the —S—S— linkages by reduction with bisulfite or thioglycol, or oxidation with performic acid. All the evidence thus indicates that the protein chain is in a highly extended state, and can only be elongated further by a small amount.

These characteristics are well accounted for by the proposed model, since the ten-chain unit is capable of a small extension but would be expected to rupture beyond this point. If we assume a 5 per cent extension of the structure to occur *via* an increase in the pitch of the basic helix, without any change in the radius, then from equation (1) we find that $\theta = 13.9^\circ$, a relatively small change from the assumed normal value of $\theta = 14.5^\circ$. This change, as can be seen from equation (3), will not require any significant change in the hydrogen bonding distance between chains. The residue length, determined from equation (2), will increase from 3.06 Å to 3.19 Å. This could be accommodated by an increase of 7° in the $C_{a1} C_{a2} C_{a3}$ angle (which corresponds quite closely to the tetrahedral angle at the C_{a2} atom), from the 107.5° of the unstretched state. While it is possible to entertain bond angle distortions of this amount, it is likely that larger distortions would not be possible without rupture of the structure. The limited extension which is observed is thus satisfactorily explained.

(b) *Effect of Water.* We have noted (1) that the intensity of the 33 Å equa-

torial reflection is extraordinarily sensitive to the water content of the sample, diminishing to zero intensity in a fully wet sample. If we assume the structure shown in Fig. 4, then it is reasonable to suppose that the water will at least enter the two 22.4 Å diameter holes in the unit cell. Taking each hole to be uniformly filled with water, we can determine its scattering factor as that of a solid cylinder, viz., $J_1(2\pi rR)/2\pi rR$. From knowledge of the amino acid composition of feather (1), we find that the ratio of the scattering from the protein cylinder to that from the water cylinder is 1.32:1. When this is used to calculate the intensity of the 33 Å reflection we find for structure A, that $F^2(110) = 23$, in comparison to 7380 for the "dry" structure. It is clear that this mechanism can readily account for the observed weakening of this spot. In an analogous fashion, the model would explain the enhancement in the intensity of this spot upon deposition of osmium (25), on the assumption that the osmium deposits primarily in the holes in the unit cell.

The slight variation in the value of this equatorial spacing between wet and dry samples, of the order of 5 per cent, is consistent with the limited swelling of the unit cell which could very likely occur as a result of the entry of water. It is interesting to note that measurements which we have made of water uptake by a sample of calamus (corrected as best as possible for condensation on the surface) indicate a weight increase of about 23 per cent. If the water entered only into the holes between the cables, the calculated increase in weight is about 19 per cent, assuming no swelling of the structure. If water also enters the hole in the center of each cylindrical unit, then this weight increase could be larger, up to about 23.5 per cent. The proposed structure can therefore account for the order of magnitude of water absorbed by feather.

(c) *Infrared Dichroism.* As was noted in an earlier section of this paper, the perpendicular dichroism of $\nu(\text{NH})$ is observed to be 4.8:1 (8). The computed dichroism of the proposed model is found to be $\frac{1}{2}\tan^2 75.5 = 7.45$, which is more than adequate to account for the observed value. The lower observed dichroism could result from the presence of a disordered component, which is indicated by the x-ray diffraction pattern (1).

(d) *Density.* The density of feather keratin has been determined to be 1.27 gm/cc (26). (The density of most fibrous proteins is about 1.3 gm/cc.) From the amino acid composition determined in this work (1), we find the mean residue weight to be 105.3. We will assume that each proline residue binds one water molecule to the free $\text{C} = \text{O}$ group. On this basis the density of a single ten-chain cylindrical unit of $r = 11.2$ Å is readily computed to be 1.54. If these units form cables and pack in the manner shown in Fig. 4, the corresponding density is found to be 1.09. The latter value is unsatisfactorily low, but several factors must be considered before rejecting the model on this basis: (1) Measurements of water uptake which we have made on feather indicate that an air-dried specimen has about 5 per cent of water as compared to a sample dried in a desiccator. Infrared spectra

also indicate that this is a reasonable estimate. This would increase the calculated density of the unit cell to 1.145. (2) No account has been taken of the disordered protein, which may comprise 25 per cent, or even more, of the specimen (1). The inclusion of some of this non-crystalline component into the holes in the crystalline structure would more than adequately raise the calculated density to the observed value. (3) If the mean residue weight is higher than the value determined here, the density would be correspondingly greater.

It is pertinent to note that even for a structure as well characterized as the α -helix density anomalies exist. Thus, while density measurements indicate an average residue volume of 140 A^3 in a sample of porcupine quill, the Pauling-Corey model predicts an average residue volume of 150 A^3 (27). Nor is the agreement improved when the α -helix is incorporated into a coiled-coil model (28, 29). We feel that the discrepancy between the observed and calculated densities of feather keratin is not severe enough to reject the proposed model, particularly since the density of the basic units is high enough and the manner of incorporation of the disordered material is not yet known.

(e) *Solubility.* The evidence on the solubilization of feather keratin indicates that a relatively homogeneous unit of molecular weight about 10,000 can be obtained in solution, the form of this unit most likely being a random coil (1). The solubilized keratin, whether in the reduced or oxidized form, can be reconstituted to give some of the main x-ray diffraction spacings of the native material.

These facts are well accounted for by the present model if we assume that the polypeptide chains are either of finite (and equal) length, or are easily ruptured at periodic intervals (*e.g.*, by the solubilization procedure). Following the assumed periodicity of proline residues, it would be most natural to surmise a related periodicity of such labile sites. If we take these to occur at every 12th proline residue, then the molecular weight of the solubilized polypeptide chain is 10,100, and it would be expected to exist in solution as a random coil. When reconstituted, the original β -helical structures are reformed with prolines still matching on neighboring chains although the alignment of ends may not be fully recovered. This accounts quite normally for the subsequent presence of the 23.6 A meridional spot in the reconstituted cysteic acid keratin. Incidentally, the reappearance of this reflection is difficult to explain if it is assumed that it arises from folds in the polypeptide chain, these folds presumably being stabilized by $-\text{S}-\text{S}-$ linkages (30, 25). The absence of the 33 A equatorial reflection in reconstituted cysteic acid keratin (30) also points to the $-\text{S}-\text{S}-$ linkages as being of importance primarily in stabilizing the lateral interactions. This would be consistent with the proposed model, since the aggregation into cables, whose packing accounts for the 33 A reflection, probably results primarily from $-\text{S}-\text{S}-$ linkages between cylindrical units.

It is not felt that the inability to detect N-terminal end groups (5) is a severe criticism of the above-postulated mechanism. If the N-terminal end group is proline,

it may be sufficiently masked in the soluble unit or difficult to detect (31). And the 1 equivalent of C-terminal amino acid per mole which is found distributed among eight different amino acids, rather than being due to an impurity (5), may represent the various C-terminal ends that can be associated with a break at a proline residue. We would conclude that the proposed structure for feather keratin encounters no unreasonable obstacle in accounting for the observed solubility properties.

SUMMARY

The structural component of feather keratin contains about 12 per cent of proline, an amount which if randomly distributed along the polypeptide chain would not be likely to give rise to the highly ordered structure which is observed in the x-ray diffraction pattern. We have found that if it is assumed that the proline residues are periodically located along the chain, it is possible for the extended chain to assume a long-pitch helical conformation, which we call a β -helix. Such helices tend to aggregate by hydrogen bonding to form cylindrical units of unique polypeptide chain structure. These units can further aggregate into cable-like structures. Preliminary investigations of this model indicate that it is better capable of explaining the sum of the data on feather keratin than any of the previously proposed structures. The model has been tested with respect to such properties as the equatorial and meridional diffraction patterns, cylindrical Patterson function, radial Fourier synthesis, elongation characteristics, density, infrared dichroism, and the effect of chemical agents. While the agreement with observation is not in all cases complete, it is satisfactory enough to suggest the proposed β -helix model as a likely basis for the structure of feather keratin.

Support is gratefully acknowledged from United States Public Health Service grants H-2740 and A-2830.

This work is based in part on a thesis submitted by R. Schor in partial fulfillment of the requirements for the Ph.D. degree, University of Michigan, 1958.

Received for publication, March 13, 1961.

REFERENCES

1. SCHOR, R., and KRIMM, S., *Biophysic. J.*, 1961, **1**, 467.
2. KRIMM, S., and SCHOR, R., *J. Chem. Physics*, 1956, **24**, 922.
3. PAULING, L., COREY, R. B., and BRANSON, H. R., *Proc. Nat. Acad. Sc.*, 1951, **37**, 205.
4. SZENT-GYORGYI, A. G., and COHEN, C., *Science*, 1957, **126**, 697.
5. WOODIN, A. M., *Biochem. J.*, 1956, **63**, 576.
6. SCHROEDER, W. A., KAY, L. M., MUNGER, N., MARTIN, N., and BALOG, J., *J. Am. Chem. Soc.*, 1957, **79**, 2769.
7. SCHROEDER, W. A., KAY, L. M., LEWIS, B., and MUNGER, N., *J. Am. Chem. Soc.*, 1955, **77**, 3901.
8. PARKER, K. D., *Biochem. et Biophysica Acta*, 1955, **17**, 148.
9. PAULING, L., and COREY, R. B., *Proc. Nat. Acad. Sc.*, 1953, **39**, 253.

10. PAULING, L., and COREY, R. B., *Proc. Nat. Acad. Sc.*, 1951, **37**, 251.
11. PAULING, L., and COREY, R. B., *Proc. Roy Soc. London, Series B*, 1953, **141**, 21.
12. PAULING, L., in *Symposium on Protein Structure*, (A. Neuberger, editor), London, Methuen and Co., 1958, 17.
13. STUART, H. A., *Die Physik der Hochpolymeren*, Berlin, Springer-Verlag, 1952, **1**.
14. DONOHUE, J., *J. Physic. Chem.*, 1952, **56**, 502.
15. PAULING, L., *Nature of the Chemical Bond*, Ithaca, Cornell University Press, 3rd edition, 1960.
16. DONOHUE, J., *Proc. Nat. Acad. Sc.*, 1953, **39**, 470.
17. LEUNG, Y. C., and MARSH, R. E., *Acta Cryst.*, 1958, **11**, 17.
18. RAMACHANDRAN, G. N., and SASISEKHARAN, V., *Arch. Biochem. and Biophysics*, 1956, **63**, 255.
19. BRAGG, W. L., and PERUTZ, M. F., *Proc. Roy. Soc. London, Series A*, 1952, **213**, 425.
20. KRIMM, S., and TIFFANY, M. L., *Biophysical Society Abstracts*, 1961, SB10.
21. BEAR, R. S., and RUGO, H. J., *Ann. New York Acad. Sc.*, 1951, **53**, 627.
22. COCHRAN, W., CRICK, F. H. C., and VAND, V., *Acta Cryst.*, 1952, **5**, 581.
23. JOHNSON, C., Ph.D. thesis, Massachusetts Institute of Technology, 1959.
24. YAKEL, H. L., and SCHATZ, P. N., *Acta Cryst.*, 1955, **8**, 22.
25. FRASER, R. D. B., and MACRAE, T. P., *J. Molecular Biol.*, 1959, **1**, 387.
26. FRASER, R. D. B., and MACRAE, T. P., *Textile Research J.*, 1957, **27**, 384.
27. FRASER, R. D. B., MACRAE, T. P., and SIMMONDS, D. H., *Biochim. et Biophysica Acta*, 1957, **25**, 654.
28. PAULING, L., and COREY, R. B., *Nature*, 1953, **171**, 59.
29. CRICK, F. H. C., *Acta Cryst.*, 1953, **6**, 689.
30. ROUGVIE, M. A., Ph.D. thesis, Massachusetts Institute of Technology, 1954.
31. ANFINSEN, C. B., and REDFIELD, R. R., *Advances in Protein Chem.*, 1956, **11**, 1.